Characterizing human skin blood flow regulation in response to different local skin temperature perturbations

Wu, Y.; Nieuwenhoff, M. D.; Huygen, F.J.P.M.; van der Helm, F. C T; Niehof, S.P.; Schouten, A. C.

DOI
10.1016/j.mvr.2016.12.007

Publication date
2017

Document Version
Final published version

Published in
Microvascular Research

Microvascular Research 111 (2017) 96–102

Contents lists available at ScienceDirect

Microvascular Research

journal homepage: www.elsevier.com/locate/ymvre

Characterizing human skin blood flow regulation in response to different local skin temperature perturbations

Y. Wu [a,*], M.D. Nieuwenhoff [b], F.J.P.M. Huygen [b], F.C.T. van der Helm [a], S. Niehof [a,b,c], A.C. Schouten [a,d]

[a] Department of Biomechanical Engineering, Delft University of Technology, Mekelweg 2, 2628CD Delft, The Netherlands
[b] Department of Anesthesiology and Pain Medicine, Erasmus MC University Medical Center, P.O. box 2040, 3000CA Rotterdam, The Netherlands
[c] Department of Information, Medical Technology and Services, Maasstad Hospital, Haastrechtstraat 7D, 3079DC Rotterdam, The Netherlands
[d] Department of Biomechanical Engineering, MIRA Institute, University of Twente, Building Zuidhorst, P.O. box 217, 7500AE Enschede, The Netherlands

ARTICLE INFO

Article history:
Received 5 October 2016
Revised 17 December 2016
Accepted 19 December 2016
Available online 21 December 2016

Keywords:
Skin blood flow
Skin temperature
Small nerve fibers
Modelling
Thermoregulation

ABSTRACT

Small nerve fibers regulate local skin blood flow in response to local thermal perturbations. Small nerve fiber function is difficult to assess with classical neurophysiological tests. In this study, a vasomotor response model in combination with a heating protocol was developed to quantitatively characterize the control mechanism of small nerve fibers in regulating skin blood flow in response to local thermal perturbation.

The skin of healthy subjects' hand dorsum ($n = 8$) was heated to 42 °C with an infrared lamp, and then naturally cooled down. The distance between the lamp and the hand was set to three different levels in order to change the irradiation intensity on the skin and implement three different skin temperature rise rates (0.03 °C/s, 0.02 °C/s and 0.01 °C/s). A laser Doppler imager (LDI) and a thermographic video camera recorded the temporal profile of the skin blood flow and the skin temperature, respectively.

The relationship between the skin blood flow and the skin temperature was characterized by a vasomotor response model. The model fitted the skin blood flow response well with a variance accounted for (VAF) between 78% and 99%. The model parameters suggested a similar mechanism for the skin blood flow regulation with the thermal perturbations at 0.03 °C/s and 0.02 °C/s. But there was an accelerated skin vasoconstriction after a slow heating (0.01 °C/s) (p-value < 0.05). An attenuation of the skin vasodilation was also observed in four out of the seven subjects during the slow heating (0.01 °C/s). Our method provides a promising way to quantitatively assess the function of small nerve fibers non-invasively and non-contact.

1. Introduction

Small nerve fibers (myelinated Aδ and unmyelinated C nerve fibers) carry multiple functions, such as temperature sensation, pain sensation and autonomic functions (Hoitsma et al., 2004). Small fiber neuropathy, a complication of diabetes and also seen in polyneuropathies of other origin, is a peripheral nerve disease that selectively affects small nerve fibers and their functions (Lacomis, 2002). Small fiber neuropathy has a huge negative impact on the quality of patients' daily life (Fink and Oaklander, 2006). Early diagnosis of small fiber neuropathy and, consequently, early treatment are crucial to slow down or even prevent the progress of small fiber neuropathy.

Currently, a gold standard is not always available for the diagnosis of small fiber neuropathy, as small nerve fibers are invisible in routine neurophysiological examination. Skin biopsy with an assessment of intra-epidermal nerve fiber density, compared with quantitative sensory testing and quantitative sudomotor axonal reflex test, has a higher sensitivity for the diagnosis of small fiber neuropathy (Sommer and Lauria, 2007), but the relation between the loss of intra-epidermal nerve fiber and the pathology of small fiber neuropathy is still unknown. Moreover, skin biopsy requires specialized laboratory and intensive labor.

Corneal confocal microscopy, quantitative sensory testing and laser Doppler techniques can also facilitate the diagnosis of small fiber neuropathy (Caselli et al., 2006; Cruccu et al., 2010; Illigens et al., 2013; Namer et al., 2013; Tavakoli et al., 2010; Vas and Rayman, 2013). However corneal confocal microscopy only assesses small fiber structure, not small fiber function. Quantitative sensory testing, particularly tests of temperature perception thresholds, is dependent on subject's thermal perception and cooperation, which may lead to biased results

Abbreviations: AU, arbitrary units; LDI, laser Doppler imager; LTI, linear time-invariant; ROI, region of interest; RRST, rise rate of the skin temperature; VAF, variance accounted for.

* Corresponding author at: Room 34-F-2-220, Mekelweg 2, 2628CD Delft, The Netherlands.
E-mail addresses: yusang.wu@tudelft.nl (Y. Wu), m.nieuwenhoff@erasmusmc.nl (M.D. Nieuwenhoff), f.huygen@erasmusmc.nl (F.J.P.M. Huygen), f.c.t.vanderhelm@tudelft.nl (F.C.T. van der Helm), s.niehof@erasmusmc.nl (S. Niehof), a.c.schouten@tudelft.nl (A.C. Schouten).

http://dx.doi.org/10.1016/j.mvr.2016.12.007

(Freeman et al., 2003). Concerns about laser Doppler techniques include limited spatial or temporal resolution and the lack of standardization in laser-Doppler image processing.

Infrared thermography, with the advantages of being non-contact, convenient and explicit, has been frequently used to investigate skin vasomotor responses in recent studies (Gazerani and Arendt-Nielsen, 2011; Nielsen et al., 2013; Sun et al., 2006). Infrared thermography measures skin temperature which is determined not only by skin blood flow but also by many other factors, such as skin tissue thermal properties, heat transfer within tissue and at the skin-environment interface, and metabolic heat generation. Therefore, combined with thermography, a physical or mathematical model is necessary to translate skin temperature into skin vasomotor physiology. Among numerous studies in this field, Pennes made a groundbreaking contribution in 1948 known as Pennes bioheat equation (Pennes, 1948). An excellent review on recently developed bioheat models is presented by Bhowmik et al. (2013). Nitzan et al. (1988) and Raamat et al. (2002) reported a good correlation between the dynamics of skin blood flow and of skin temperature with modified thermal clearance method. Skin temperature curve can also provide information on skin blood flow as well as other tissue physiology (Bandini et al., 2013; Merla et al., 2002; Renkielska et al., 2006).

Small nerve fibers regulate local skin blood flow to control local skin temperature. The regulation process involves a number of different factors including TRPV-1 channels and the release of calcitonin-gene related peptide and/or substance P (Holzer, 1992; Wong and Fieger, 2010). A sustained heating at 42 °C induces a fast and initial increase of the skin blood flow in about 10 min, by exciting the axon reflex of small nerve fibers to release vasoactive peptides (Charkoudian et al., 2002; Minson et al., 2001; Pergola et al., 1993). The initial increase of the skin blood flow is relatively small when the local skin temperature remains below 35 °C, becomes significant for the skin temperatures above 37 °C and reaches a peak at around 42 °C (Barcroft and Edholm, 1943; Magerl and Treede, 1996).

Identification of the control mechanism of small nerve fiber for regulating skin blood flow response is a promising way to quantitatively assess the functionality of small nerve fibers. Few studies were conducted in this field. Mariotti et al. (2009) used a hypothetical control model to discriminate the presence of Raynaud's phenomenon, which is a condition with excessive reduction of skin blood flow in response to a thermal or emotional stress. Besides, small-fiber-regulated skin vasodilation is influenced by local heating rate, and a fast heating induces an increasing skin vasodilation (Hodges et al., 2009).

Nieuwenhoff et al. (2016) developed an experimental setup in which non-contact heating with an infrared lamp evokes small-fiber-mediated skin vasodilation. In this study, the same setup was used. The aim of this study was to 1) develop a quantitative control model which can characterize the mechanism of small nerve fibers for regulating the skin blood flow in response to a local thermal perturbation, and 2) test the hypothesis that the model parameters would change when different local thermal perturbations are applied, indicating a varying skin blood flow regulation mechanism.

2. Methods

2.1. Subjects

Ten healthy subjects (5 men and 5 women, age: 27.2 ± 2.8 years, height: 1.75 ± 0.13 m, weight: 68.4 ± 14.4 kg, values are mean ± standard deviation) participated in the study. All subjects were free of any conditions which may affect skin vasomotor response, such as neurological or vascular disorders. Before the experiment, the subjects were informed on the experimental protocol, and signed informed consent. The experiment was approved by Human Research Ethics Committee of Delft University of Technology, Delft, The Netherlands.

The subjects were requested to refrain from smoking, caffeine and alcohol for at least 8 h before the experiment, and to avoid the use of lotion, gel, cream or cosmetics on the left hand on the day of the experiment. The dorsum of the left hand was visually inspected to be free of skin injuries or scars. All accessories that may obstruct the experiment (such as rings, bracelets and watches) were removed.

2.2. Experimental setup

Fig. 1 gives an overview of the experimental setup. The experiment was performed in a temperature-controlled room (22–25 °C) with steady room illumination. The subject's left hand was heated with an infrared lamp approved for clinical use (Hydrosun 750 with optical filter Schott BG780; Hydrosun Medizintechnik GmbH, Mullheim, Germany). The emitted infrared wavelength ranged between 780 and 1400 nm and the axial irradiance was 4400 W/m^2. The lamp's heating field was centered at the dorsum of the subject's hand, and the distance between the hand and the lamp was varied according to the experimental protocol.

A laser Doppler imager (LDI) (PeriScan PIM3 System; Perimed AB, Jarfalla, Sweden) measured skin blood flow in arbitrary units (AU). The region of interest (ROI) of the LDI was a 5.0 × 5.0 cm area, centered at the hand dorsum, with a resolution of 3 mm and total 17 × 17 pixels. The frame rate was around 10 s per frame (i.e. a scan rate of ~35 ms per pixel).

The skin temperature was measured with a thermographic video camera (FLIR SC5600, FLIR System Inc., Wilsunville, USA) at a frame rate of 5 Hz and a resolution of 640 × 512 pixels. The skin emissivity was set at 0.98 (Steketee, 1973). The detectable temperature range was 5–57 °C with a resolution of 0.02 °C. The skin temperature at the dorsum center was monitored in real-time (Altair, FLIR System Inc., Wilsunville, USA). The ROI in the thermography was a quadrangle of which the corners were marked by four markers (Fig. 1).

2.3. Protocol

The timeline of the protocol is presented in Fig. 2. In each measurement the skin temperature and the skin blood flow were recorded simultaneously. The subjects acclimated to the room environment for at least 15 min before the start of the first measurements. The distance between the hand and the infrared lamp was set 20 cm in the first and the second measurement (M20(1) and M20(2), respectively). The increase of the skin temperature was significantly affected by the radiation flux from the infrared lamp, and the radiation flux on the skin was related to the distance between the lamp and the skin. In order to obtain different thermal perturbations, the hand-lamp distance was set 25 cm and 30 cm in the third (M25) and the fourth (M30) measurement, respectively.

In each measurement a 1 min baseline was recorded before the lamp was switched on to heat the skin (heating phase). The lamp was switched off when the skin temperature at the dorsum center reached 42 °C. Thereafter the measurement continued for 5 min to let the skin naturally cool down (cooling phase).

2.4. Data processing

Data were analyzed using custom-made scripts written in Matlab (Matlab R2013a, the Mathworks, Natrick, USA). In the following context the skin temperature and the skin blood flow respectively refer to the mean skin temperature and the mean skin blood flow over the pixels in the ROI, unless stated otherwise.

The baselines of the skin temperature and the skin blood flow were obtained by averaging the signals in the 1 min before the heating phase. Relative skin blood flow was defined as the skin blood flow normalized to the baseline. The heating time was obtained by visually inspecting the video thermography, as the start and the end of the heating were accompanied by an abrupt change in the skin temperature. The rise rate

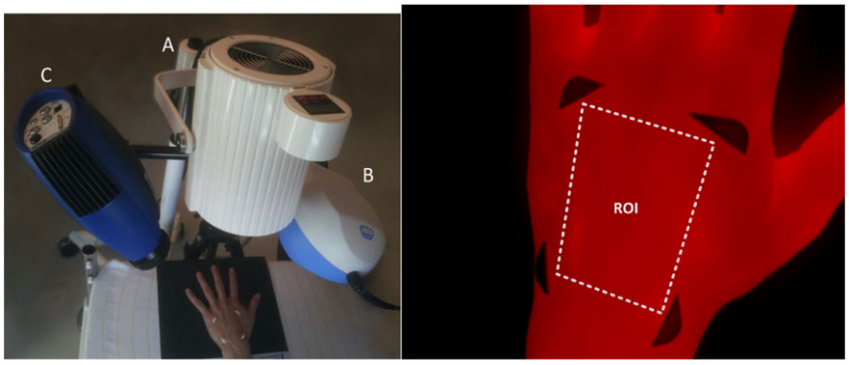

Fig. 1. Left: Overview of the experimental setup. The subject put the left hand on the table. The hand dorsum was heated with an infrared lamp (A: Hydrosun 750). A laser Doppler imager (B: PeriScan PIM3) measured skin blood flow, and the skin temperature was recorded with a thermographic video camera (C: FLIR SC5600). Right: A thermographic image. The region of interest (ROI) was a quadrangle of which the corners were defined by four markers, respectively.

of the skin temperature (RRST) was defined as the total skin temperature increment in the heating phase divided by the heating time.

2.5. Vasomotor response model

Fig. 3 shows the structure of the vasomotor response model, with the skin temperature as input and the modeled relative skin blood flow as output. A Heaviside function represents a temperature threshold for the excitation of the small nerve fibers.

$$\mu(t) = \begin{cases} 0 & T(t) \le T_{thre} \\ 1 & T(t) > T_{thre} \end{cases} \quad (1)$$

where T is the skin temperature, t time, T_{thre} the temperature threshold. $\mu = 1$ means the excitation of the small nerve fibers.

The skin blood flow response is assumed to be affected by the excitation of the small nerve fibers and the skin temperature increment over the threshold temperature. An interim variable $\varphi(t)$ is thus generated:

$$\varphi(t) = \Delta T(t) \times \mu(t) = [T(t) - T_{thre}] \times \mu(t) \quad (2)$$

$\varphi(t)$ is passed to a first order linear time-invariant (LTI) subsystem with a different time constant for the heating phase and the cooling phase, respectively. The transfer function of the LTI subsystem is:

$$\frac{\hat{V}(s)}{\varphi(s)} = \frac{G}{s\tau + 1} \text{ and } \begin{cases} \tau = \tau_{heat} \text{ in the heating phase} \\ \tau = \tau_{cool} \text{ in the cooling phase} \end{cases} \quad (3)$$

in which $\hat{V}$ is the modeled relative skin blood flow, G the gain of the LTI subsystem, τ_{heat} the time constant for the heating phase, τ_{cool} the time constant for the cooling phase, and s the Laplace transform variable.

The values of the model parameters were determined by fitting the modeled relative skin blood flow to the measured relative skin blood flow using a least-squares criterion function:

$$J(\theta) = \min \frac{1}{n} \sum_{i=1}^{n} \left[V(t_i) - \hat{V}(\theta, t_i) \right]^2 \quad (4)$$

in which n is the number of the samples, θ the parameter vector including T_{thre}, G, τ_{heat} and τ_{cool}. $V(t_i)$ is the relative skin blood flow measured at time t_i, and $\hat{V}(\theta, t_i)$ the modeled relative skin blood flow with the parameter vector θ at time t_i.

Variance accounted for (VAF) was used to quantify the quality of the fitting. The VAF was defined as:

$$VAF = \left(1 - \frac{var\left(V - \hat{V}\right)}{var(V)} \right) \times 100\% \quad (5)$$

where var. is an operator of variance.

2.6. Statistics

Results are presented as mean over the subjects with the standard deviation (mean ± SD). Differences in the skin temperature, the skin blood flow and the RRST between the measurements were analyzed with repeated measures ANOVA and Bonferroni correction. The quartile values of the VAFs in all the measurements was defined with the method of Tukey's Hinges. The quality of the model fitting in a measurement was considered weak when the VAF was >1.5 inter-quartile ranges

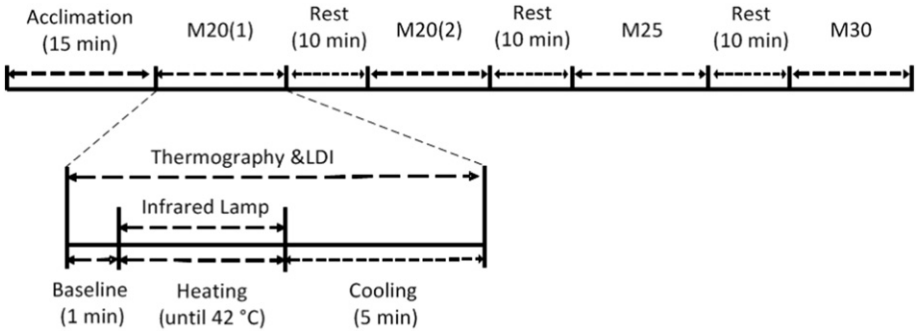

Fig. 2. Timeline of the experimental protocol. After 15 min acclimation a 1 min baseline was recorded before the lamp was switched on to heat the skin (heating phase). The lamp was switched off when the skin temperature at the dorsum center reached 42 °C. Thereafter the measurement continued for 5 min to let the skin naturally cool down (cooling phase). The subjects relaxed for 10 min between two measurements.

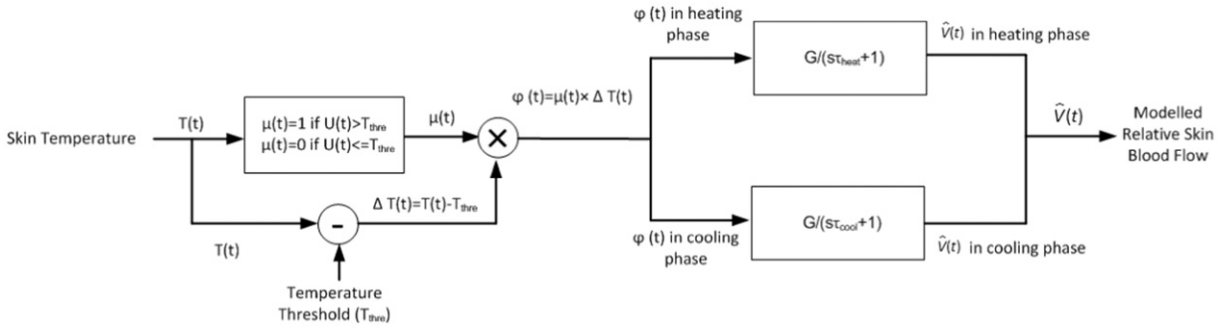

Fig. 3. The vasomotor response model structure. The input of the model is the measured skin temperature, and the output is the modeled relative skin blood flow. The model consists of a temperature threshold in series with a first order linear time-invariant (LTI) subsystem, where two different time constants are used for the heating phase and the cooling phase, respectively. The values of the model parameters were determined by fitting the modeled relative skin blood flow to the measured relative skin blood flow using a least-squares criterion function.

below the lower quartile, and the model parameters in that measurement were excluded from further analysis. Differences in the model parameters between the measurements were analyzed with Friedman Test and a Bonferroni correction. Post hoc analysis was conducted with Wilcoxon signed-rank tests. p-Values smaller than 0.05 were considered statistically significant.

3. Results

Fig. 4 shows the skin temperature and the skin blood flow of one subject in a measurement. The increase of the skin blood flow lagged behind the increase of the skin temperature, and the skin blood flow reached a peak in the cooling phase when the skin temperature was already declining. The responses of the skin temperature and skin blood flow of all the subjects were visually inspected. Two subjects (subject ID: S04 & S10) had different and anomalous responses compared with the other eight subjects. The data of these two subjects were excluded from the further analysis. S04 had a long heating phase (>10 min) in all the measurements, but the skin temperature at the dorsum center always reached a plateau below 42 °C. The skin blood flow of S04 increased in the heating phase, but remained high and did not return to the baseline in the cooling phase. S10 had a relatively minor and short response of the skin blood flow mixed with large noises.

Table 1 presents the overview of the skin temperature, the skin blood flow and the RRST over the subjects ($n = 8$). The infrared lamp was switched off when the mean skin temperature at the dorsum center reached 42 °C. The peak of the mean skin temperature over the ROI was just below 42 °C, as the ROI was larger than the dorsum center area. There were no significant differences in the skin temperature between any two measurements. The peak skin blood flow in M20(1) was significantly higher than that in M30 (p-value < 0.05).

The change in the hand-lamp distance resulted in significant differences in the RRST (p-value < 0.01). The RRSTs in M20(1) and M20(2) were significantly higher than the RRST in M25 (M20(1) vs. M25: p-value < 0.05; M20(2) vs. M25: p-value < 0.01). The RRSTs in M20(1), M20(2) and M25 were significantly higher than the RRST in M30 (p-value < 0.01 in all the comparisons). No significant differences in the RRST were found between M20(1) and M20(2).

Fig.5 shows the relationship between the skin blood flow and the skin temperature. In the heating phase, the skin blood flow started rising when the skin temperature was around 39 °C. In the cooling phases of M20(1), M20(2) and M25, the skin blood flow reached a plateau, remained high until the skin temperature dropped to 39–40 °C, and

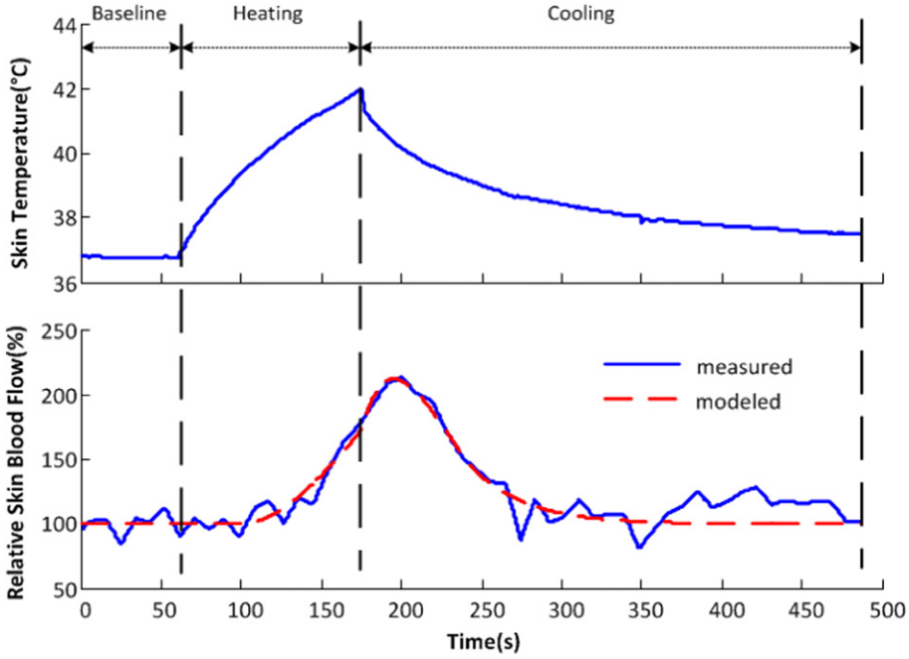

Fig. 4. The skin temperature and the skin blood flow (solid lines) of one subject in M20(2). The skin blood flow is normalized to the baseline. The modeled skin blood flow (dashed line), i.e. the output of the vasomotor response model, is also presented.

Table 1
Overview of the skin temperature, the skin blood flow and the RRST over the subjects ($n = 8$).

		M20(1)	M20(2)	M25	M30
Skin temperature	Baseline (°C)	35.9 ± 1.0	36.2 ± 0.8	35.9 ± 0.9	35.9 ± 0.9
	Peak (°C)	41.4 ± 0.3	41.4 ± 0.4	41.5 ± 0.3	41.3 ± 0.4
Skin blood flow	Baseline (AU)	82.6 ± 38.1	90.2 ± 40.3	74.9 ± 29.6	69.7 ± 23.3
	Peak (AU)	306 ± 77	265 ± 110	269 ± 92	222 ± 73*
RRST (°C/s)		0.027 ± 0.009	0.030 ± 0.010	0.020 ± 0.006*, **	0.012 ± 0.004†

* p-Value < 0.05 compared with M20(1).
** p-Value < 0.01 compared with M20(2).
† p-Value < 0.01compared with M20(1), M20(2) and M25.

then subsided quickly. In the cooling phase of M30, the plateau of the skin blood flow was shorter.

An example of the fitting to the measured skin blood flow response with the vasomotor response model is shown in Fig. 4. The results of the model fitting are listed in Table 2. In 31 out of 32 measurements, the VAFs were in a range from 78% to 99%, indicating a good fitting quality. In the comparisons of the model parameters between the measurements, the τ_{cool} in M30 was significantly lower than the τ_{cool} in M20(2) and M25 (p-value < 0.05 in the both comparisons). Moreover, M30 had the lowest gain in four out of the seven subjects.

4. Discussion

This study developed a quantitative method to describe the control mechanism of small nerve fibers for regulating skin blood flow in response to an external thermal perturbation. The skin blood flow response in our study was mainly regulated by the small nerve fibers, as the heating time (3–10 min) and the heated skin temperature (~42 °C) were close to the conditions in the previous study, which indicated small nerve fibers as a main contributor to local skin blood flow regulation (Minson et al., 2001). The increase of the skin temperature was considered as a key factor in exciting small nerve fibers and thereafter inducing skin blood flow response.

In this study the heating intensity was adjusted by changing the distance of the lamp from the skin, which resulted in different RRST. The skin blood flow regulation process was characterized by the four parameters in our vasomotor response model. The temperature threshold indicates at which skin temperature level the skin blood flow begins to increase. The gain indicates the amplitude when the skin blood flow reaches a steady state. A lower gain indicates an attenuation in the skin vasodilation. The τ_{heat} and the τ_{cool} inversely and respectively indicate the change rate of the skin blood flow response in the heating and cooling phase (i.e. a high τ means a slow change and a low τ means a fast change). With similar skin temperature perturbations for one hand-lamp distance, the temporal profile of the skin blood flow response had a large variation over the subjects, and three of the four model parameters (gain, τ_{heat} and τ_{cool}) had relatively high standard deviations over the subjects.

The comparisons of the model parameters between the measurements suggested a similar mechanism for the skin blood flow regulation in M20(1), M20(2) and M25. However, with the slowest RRST, the skin blood flow regulation in M30 appeared to be different (Fig. 5). The lower τ_{cool} in M30 indicated a faster skin vasoconstriction in the cooling phase. Besides, although no significant differences were found, M30 had the lowest gain compared with the other three measurements in four out of the seven subjects. Hodges et al. (2009) reported that axon-reflex-mediated skin vasodilation at a heating rate of 0.1 °C/min

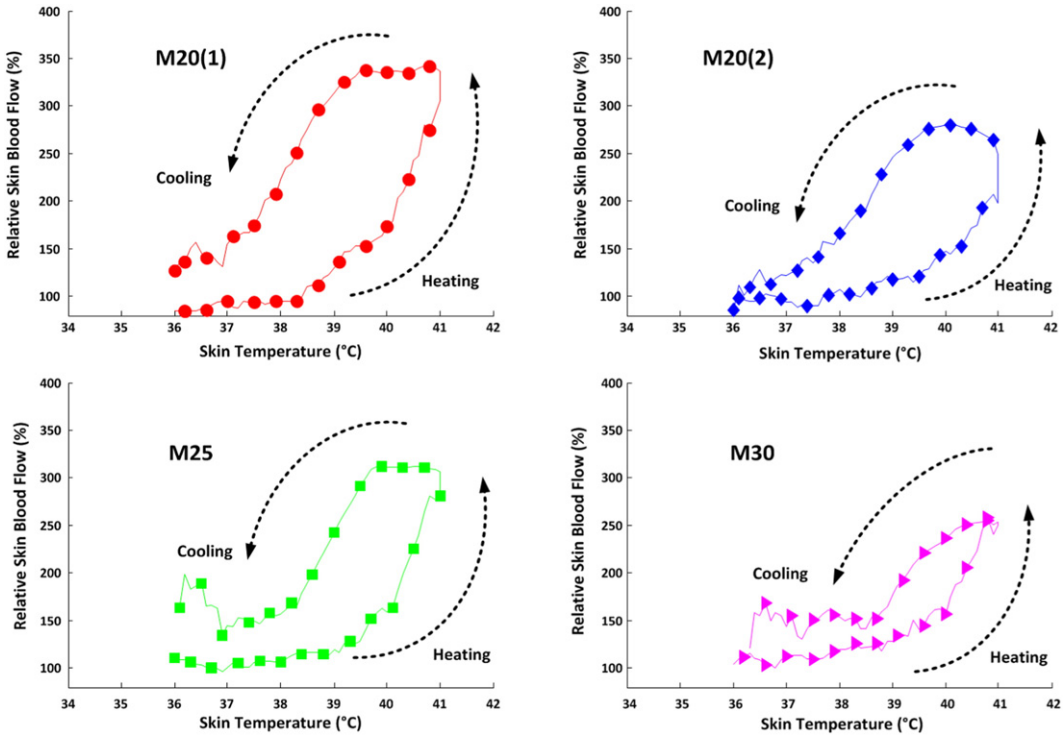

Fig. 5. The (relative) skin blood flow is plotted against the skin temperature in the four measurements. The (relative) skin blood flow and the skin temperature are averaged over the subjects ($n = 8$).

Table 2
Overview of the fitted model parameters and the VAF.

	M20(1)	M20(2)	M25	M30
Number of subjects	8	8	8	7[a]
T_{thre} (°C)	38.0 ± 1.18	38.4 ± 1.26	38.3 ± 1.18	37.8 ± 1.45
Gain (AU)	1.57 ± 0.89	2.24 ± 2.18	1.50 ± 0.73	0.84 ± 0.44
τ_{heat} (s)	86.00 ± 77.35	144.09 ± 92.66	129.66 ± 128.90	76.26 ± 52.75
τ_{cool} (s)	47.00 ± 31.86	44.61 ± 22.28	41.49 ± 23.56	22.45 ± 20.02[†]
VAF (%)	94.10 ± 4.31	93.78 ± 4.16	92.42 ± 5.30	81.19 ± 9.54

[a] The model results in one measurement were excluded as outliers. The VAF in this measurement was 61.4%.
[†] p-Value < 0.05 compared with M20(2) and M25.

(0.0017 °C/s) was significantly attenuated compared with the skin vasodilation at 2 °C/min (0.033 °C/s). A fast and (potentially) noxious perturbation likely triggers a protective mechanism by extensively increasing skin blood flow. In our study, the attenuation of the skin vasodilation was not significant probably due to the relatively narrow range of the RRST (0.01–0.03 °C/s). Hodges et al. (2009) also reported that the effects of heating rate on skin blood flow response extended beyond the heating period. It may explain the acceleration of the skin vasoconstriction in the cooling phase with a slower RRST.

The model was constructed based on the observations in this study as well as previous studies. First, there is certain temperature threshold for the onset of the skin blood flow response (Magerl and Treede, 1996; Nieuwenhoff et al., 2016). The temperature threshold mechanism can be also seen in Fig.5. Secondly, different bio-chemical interactions were assumed to exist in the heating phase and the cooling phase, which successively determined the profile of the skin blood flow response. In order to reduce the model complexity, a first-order LTI subsystem with two time constants respectively for the heating and cooling phase was applied. Thirdly, an open loop structure was applied in our model as the effects of the skin blood flow on the skin temperature was assumed negligible. Petrofsky et al. (2011) found little effects of skin blood flow on skin temperature when the skin blood flow was occluded during local skin warming. Wilson and Spence (1988) applied a heat transfer model to simulate skin temperature response to a cold perturbation on forearm, and found that the initial skin temperature recovery was predominantly determined by the thermal properties of the skin tissue rather than the skin blood flow. Further study is required to obtain the quantitative knowledge on physiological process of skin blood flow regulation, and to make a better correspondence between the model and the actual process.

Our methods are non-contact, non-invasive and can be helpful to quantitatively identify the function of small nerve fibers in clinical practice. As only hands of young subjects were studied, cautions should be taken to extrapolate these results to other body regions and older subjects. The next step will be to apply the methods in patients with small fiber neuropathy who likely have an altered small-nerve-fiber-regulated skin blood flow response and subsequently different model parameter values compared with healthy subjects.

In summary, the skin blood flow response can be quantitatively characterized with our vasomotor response model. The skin blood flow regulation can be affected by the intensity of the thermal perturbation. As the skin blood flow response in this study was mainly regulated by the small nerve fibers, further studies based on our proposed methodology may provide a non-invasive and quantitative way to help the diagnosis of small fiber neuropathy.

Author's contribution

YW collected the data and drafted the manuscript. YW and MN were involved in the design of the experiments, the data analysis and the data interpretation. MN, FH and FvdH critically revised the manuscript. SN and AS conceived the study, participated in the data analysis and the data interpretation, and helped to draft the manuscript. All authors read and approved the final manuscript.

Conflicts of interest

No benefits in any form have been or will be received from a commercial party related directly or indirectly to the subject of this manuscript.

Acknowledgments

This research is supported by the Dutch Technology Foundation STW (grant 10730), which is part of the Netherlands Organization for Scientific Research (NWO) which is partly funded by the Ministry of Economic Affairs. Noldus Information Technology, FLIR and the Centre for Human Drug Research Leiden (CHDR) contributed to this project via the Dutch Technology Foundation STW. For this study the thermographic video camera was provided by FLIR, and the Hydrosun lamp was donated by the Erwin Braun Foundation in Basel, Switzerland.

References

Bandini, A., Orlandi, S., Manfredi, C., Evangelisti, A., Barrella, M., Bevilacqua, M., Bocchi, L., 2013. Effect of local blood flow in thermal regulation in diabetic patient. Microvasc. Res. 88, 42–47.
Barcroft, H., Edholm, O.G., 1943. The effect of temperature on blood flow and deep temperature in the human forearm. J. Physiol. 102 (1), 5–20.
Bhowmik, A., Singh, R., Repaka, R., Mishra, S.C., 2013. Conventional and newly developed bioheat transport models in vascularized tissues: a review. J. Therm. Biol. 38 (3), 107–125.
Caselli, A., Spallone, V., Marfia, G.A., Battista, C., Pachatz, C., Veves, A., Uccioli, L., 2006. Validation of the nerve axon reflex for the assessment of small nerve fibre dysfunction. J. Neurol. Neurosurg. Psychiatry 77 (8), 927–932.
Charkoudian, N., Eisenach, J.H., Atkinson, J.L.D., Fealey, R.D., Joyner, M.J., 2002. Effects of chronic sympathectomy on locally mediated cutaneous vasodilation in humans. J. Appl. Physiol. 92 (2), 685–690.
Cruccu, G., Sommer, C., Anand, P., Attal, N., Baron, R., Garcia-Larrea, L., Haanpaa, M., Jensen, T.S., Serra, J., Treede, R.D., 2010. EFNS guidelines on neuropathic pain assessment: revised 2009. Eur. J. Neurol. 17 (8), 1010–1018.
Fink, E., Oaklander, A.L., 2006. Small-fiber neuropathy: answering the burning questions. Sci. SAGE KE 2006 (6), pe7.
Freeman, R., Chase, K.P., Risk, M.R., 2003. Quantitative sensory testing cannot differentiate simulated sensory loss from sensory neuropathy. Neurology 60 (3), 465–470.
Gazerani, P., Arendt-Nielsen, L., 2011. Cutaneous vasomotor reactions in response to controlled heat applied on various body regions of healthy humans: evaluation of time course and application parameters. Int. J. Physiol. Pathophysiol. Pharmacol. 3 (3), 202–209.
Hodges, G.J., Kosiba, W.A., Zhao, K., Johnson, J.M., 2009. The involvement of heating rate and vasoconstrictor nerves in the cutaneous vasodilator response to skin warming. Am. J. Physiol. Heart Circ. Physiol. 296 (1), H51–H56.
Hoitsma, E., Reulen, J.P.H., de Baets, M., Drent, M., Spaans, F., Faber, C.G., 2004. Small fiber neuropathy: a common and important clinical disorder. J. Neurol. Sci. 227, 119–130.
Holzer, P., 1992. Peptidergic sensory neurons in the control of vascular functions: mechanisms and significance in the cutaneous and splanchnic vascular beds. Rev. Physiol. Biochem. Pharmacol. 121, 49–146.
Illigens, B.M., Siepmann, T., Roofeh, J., Gibbons, C.H., 2013. Laser Doppler imaging in the detection of peripheral neuropathy. Auton. Neurosci. 177 (2), 286–290.
Lacomis, D., 2002. Small-fiber neuropathy. Muscle Nerve 26 (2), 173–188.
Magerl, W., Treede, R.D., 1996. Heat-evoked vasodilatation in human hairy skin: axon reflexes due to low-level activity of nociceptive afferents. J. Physiol. 497 (3), 837–848.
Mariotti, A., Grossi, G., Amerio, P., Orlando, G., Mattei, P.A., Tulli, A., Romani, G.L., Merla, A., 2009. Finger thermoregulatory model assessing functional impairment in Raynaud's phenomenon. Ann. Biomed. Eng. 37 (12), 2631–2639.
Merla, A., Di Donato, L., Di Luzio, S., Romani, G.L., 2002. Quantifying the relevance and stage of disease with the Tau image technique. IEEE Eng. Med. Biol. Mag. 21 (6), 86–91.
Minson, C.T., Berry, L.T., Joyner, M.J., 2001. Nitric oxide and neurally mediated regulation of skin blood flow during local heating. J. Appl. Physiol. 91 (4), 1619–1626.

Namer, B., Pfeffer, S., Handwerker, H.O., Schmelz, M., Bickel, A., 2013. Axon reflex flare and quantitative sudomotor axon reflex contribute in the diagnosis of small fiber neuropathy. Muscle Nerve 47 (3), 357–363.

Nielsen, T.A., da Silva, L.B., Arendt-Nielsen, L., Gazerani, P., 2013. The effect of topical capsaicin-induced sensitization on heat-evoked cutaneous vasomotor responses. Int. J. Physiol. Pathophysiol. Pharmacol. 5 (3), 148–160.

Nieuwenhoff, M.D., Wu, Y., Huygen, F., Schouten, A., van der Helm, F., Niehof, S.P., 2016. Reproducibility of axon reflex-related vasodilation assessed by dynamic thermal imaging in healthy subjects. Microvasc. Res. 106, 1–7.

Nitzan, M., Fairs, S.L., Roberts, V., 1988. Simultaneous measurement of skin blood flow by the transient thermal-clearance method and laser Doppler flowmetry. Med. Biol. Eng. Comput. 26 (4), 407–410.

Pennes, H.H., 1948. Analysis of tissue and arterial blood temperatures in the resting human forearm. J. Appl. Physiol. 1 (2), 93–122.

Pergola, P.E., Kellogg, D.L., Johnson, J.M., Kosiba, W.A., Solomon, D.E., 1993. Role of sympathetic nerves in the vascular effects of local temperature in human forearm skin. Am. J. Physiol. Heart Circ. Physiol. 265 (3), H785–H792.

Petrofsky, J., Paluso, D., Anderson, D., Swan, K., Yim, J.E., Murugesan, V., Chindam, T., Goraksh, N., Alshammari, F., Lee, H., 2011. The contribution of skin blood flow in warming the skin after the application of local heat; the duality of the Pennes heat equation. Med. Eng. Phys. 33 (3), 325–329.

Raamat, R., Jagomägi, K., Kingisepp, P.H., 2002. Simultaneous recording of fingertip skin blood flow changes by multiprobe laser Doppler flowmetry and frequency-corrected thermal clearance. Microvasc. Res. 64 (2), 214–219.

Renkielska, A., Nowakowski, A., Kaczmarek, M., Ruminski, J., 2006. Burn depths evaluation based on active dynamic IR thermal imaging—a preliminary study. Burns 32 (7), 867–875.

Sommer, C., Lauria, G., 2007. Skin biopsy in the management of peripheral neuropathy. Lancet Neurol. 6, 632–642.

Steketee, J., 1973. Spectral emissivity of skin and pericardium. Phys. Med. Biol. 18 (5), 686.

Sun, P.C., Lin, H.D., Jao, S.H., Ku, Y.C., Chan, R.C., Cheng, C.K., 2006. Relationship of skin temperature to sympathetic dysfunction in diabetic at-risk feet. Diabetes Res. Clin. Pract. 73 (1), 41–46.

Tavakoli, M., Marshall, A., Pitceathly, R., Fadavi, H., Gow, D., Roberts, M.E., Efron, N., Boulton, A.J., Malik, R.A., 2010. Corneal confocal microscopy: a novel means to detect nerve fibre damage in idiopathic small fibre neuropathy. Exp. Neurol. 223 (1), 245–250.

Vas, P.R., Rayman, G., 2013. The rate of decline in small fibre function assessed using axon reflex-mediated neurogenic vasodilatation and the importance of age related centile values to improve the detection of clinical neuropathy. PLoS One 8 (7), e69920.

Wilson, S.B., Spence, V.A., 1988. A tissue heat transfer model for relating dynamic skin temperature changes to physiological parameters. Phys. Med. Biol. 33 (8), 895.

Wong, B.J., Fieger, S.M., 2010. Transient receptor potential vanilloid type-1 (TRPV-1) channels contribute to cutaneous thermal hyperaemia in humans. J. Physiol. 588, 4317–4326.